The Journal of Neuroscience, May 1, 2001, 21(9):3009–3016

$GABA_A$ Receptor α1 Subunit Deletion Prevents Developmental Changes of Inhibitory Synaptic Currents in Cerebellar Neurons

Stefano Vicini,[1] Carolyn Ferguson,[2] Kate Prybylowski,[1] Jason Kralic,[3] A. Leslie Morrow,[3] and Gregg E. Homanics[2]

[1]Department of Physiology and Biophysics, Georgetown University Medical School, Washington, DC 20007, [2]Departments of Anesthesiology/Critical Care Medicine and Pharmacology, University of Pittsburgh, Pittsburgh, Pennsylvania 15261, and [3]Department of Psychiatry and Pharmacology, University of North Carolina Medical School, Chapel Hill, North Carolina 27599-7178

Developmental changes in miniature IPSC (mIPSC) kinetics have been demonstrated previously in cerebellar neurons in rodents. We report that these kinetic changes in mice are determined primarily by developmental changes in $GABA_A$ receptor subunit expression. mIPSCs were studied by whole-cell recordings in cerebellar slices, prepared from postnatal day 11 (P11) and P35 mice. Similar to reports in granule neurons, wild-type cerebellar stellate neuron mIPSCs at P11 had slow decay kinetics, whereas P35 mIPSCs decayed five times faster. When mIPSCs in cerebellar stellate neurons were compared between wild-type (+/+) and $GABA_A$ receptor α1 subunit-deficient (−/−) littermates at P35, we observed dramatically slower mIPSC decay rates in −/− animals. We took advantage of the greater potency of imidazopyridines for GABA current potentiation with α1 subunit-containing receptors to characterize the relative contribution of α1 subunits in native receptors on inhibitory synapses of cerebellar granule neurons. Zolpidem-induced prolongation of mIPSC decay was variable among distinct cells, but it increased during development in wild-type mice. Similarly, Zolpidem prolongation of mIPSC decay rate was significantly greater in adult +/+ mice than in knock-outs. We propose that an increased α1 subunit assembly in postsynaptic receptors of cerebellar inhibitory synapses is responsible for the fast inhibitory synaptic currents that are normally observed during postnatal development.

Key words: GABA receptor; gene knock-out; patch-clamp; inhibitory synapses; development; GABA

Spontaneous IPSCs (sIPSCs) and miniature IPSCs (mIPSCs) [recorded in the presence of tetrodotoxin (TTX)] in mammalian neurons have been shown to become faster with development (Brickley et al., 1996; Draguhn and Heinemann, 1996; Tia et al., 1996; Brussard et al., 1997; Hollrigel and Soltesz, 1997; Pouzat and Hestrin, 1997; Dunning et al., 1999; Okada et al., 2000). Several mechanisms have been proposed to explain these changes, including changes in expression of specific $GABA_A$ receptor ($GABA_A$-R) subunits (Tia et al., 1996; Dunning et al., 2000; Okada et al., 2000) and changes in reuptake mechanisms (Draguhn and Heinemann, 1996). Recent studies with overexpression of the α1 subunit of the $GABA_A$ receptor in thalamic neurons have indicated that the enhanced expression of the α1 subunit could be responsible for faster mIPSCs (Okada et al., 2000). This hypothesis is supported by work in recombinant systems that demonstrate that rapid application of brief pulses of GABA to outside-out excised patches generates faster currents with $\alpha1\beta2\gamma2$ than with other subunit combinations (Verdoorn, 1994; Gingrich et al., 1995; Lavoie et al., 1997; McClellan and Twyman, 1999).

sIPSCs have been characterized extensively in granule and stellate neurons in rat cerebellar slices (Llano and Gerschenfeld, 1993; Brickley et al., 1996, 1999; Tia et al., 1996; Nusser et al., 1997; Kondo and Marty, 1998). The decay time of sIPSCs in granule neurons has been shown to undergo a developmental decrease (Brickley et al., 1996; Tia et al., 1996). Whereas in granule neurons many distinct subunits are expressed, in stellate neurons, mRNAs have been found only for the α1, β2, and γ2 subunits of the $GABA_A$ receptor, although low levels of mRNA for α2 and α3 subunits were seen early in development (Laurie et al., 1992a,b). It is therefore of interest to assess whether developmental changes of mIPSC kinetics can be observed in stellate neurons that should therefore express a more restricted number of receptor subtypes.

In situ hybridization studies have shown a selective increase with development of α1 and the α6 subunits in the total cerebellum (Bovolin et al., 1992; Laurie et al., 1992b). However, the developmental changes of sIPSCs kinetics also occurred in granule cells in mutant mice lacking α6 (Farrant et al., 1999). Our aim was to investigate the role of the α1 subunit in kinetic changes of mIPSCs in developing cerebellar stellate and granule neurons using mutant mice lacking this subunit. To further support that these changes are related to the relative contributions of the α1 subunit, we studied the sensitivity of mIPSCs to the imidazopyridine Zolpidem, which has been shown to have selectivity for the benzodiazepine type 1 receptor that contains α1 subunits (Pritchett et al., 1989; MacDonald and Olsen, 1994).

MATERIALS AND METHODS

Mutant mouse production. A 775bp *Bst*EII-*Bsp*EI fragment of the bovine $GABA_A$ receptor α1 subunit cDNA (Schofield et al., 1987) was used to

Received Nov. 20, 2000; revised Feb. 15, 2001; accepted Feb. 20, 2001.

This work was supported by National Institutes of Health Grants MH01680 (S.V.), AA10422 and GM52035 (G.E.H.), and AA09013 (A.L.M.). We thank Gail Martin for generously providing actin-cre mice, and Joanne Steinmiller, Karen Renzi, Brian Sloat, JianHong Luo, and Ed Mallick for expert technical support.

Correspondence should be addressed to Dr. Stefano Vicini, Department of Physiology and Biophysics, Georgetown University School of Medicine, 3900 Reservoir Road NW, Washington, DC 20007. E-mail svicin01@georgetown.edu.

screen a strain 129/SvJ mouse genomic DNA BAC library (Genome Systems, St. Louis, MO) for the murine α1 subunit. From one of these BAC clones, a ~13 kb *Bam*HI fragment was subcloned and characterized. This clone contained an exon that corresponded to nucleotides 1307–1509 of the mouse cDNA (Keir et al., 1991). This genomic clone was used to create the targeting construct illustrated in Figure 1*A*. The selectable marker gene PGKneoNTRtkpA (Wu et al., 1994) was flanked by *lox*P sites (Sternberg and Hamilton, 1981) and inserted into an *Eco*RV site ~0.6 kb upstream of the exon. An oligonucleotide that harbored an *Eco*RI site and an additional *lox*P site was inserted into a *Bgl*II site ~0.8 kb downstream of the exon. This construct was linearized in the vector backbone with *Pvu*I and electroporated into R1 mouse embryonic stem (ES) cells (Nagy et al., 1990) as described previously (Homanics et al., 1997). ES cell clones surviving G418 selection (270 μg/ml; Life Technologies, Gaithersburg, MD) were screened for gene targeting by Southern blot analysis of genomic DNA after digestion with *Eco*RI. Blots were hybridized with probe C (see Fig. 1*A*, *C*), which is external to the targeting construct.

The selectable marker cassette was removed *in vitro* from two ES cell clones that were correctly targeted. To accomplish this, these clones were transiently transfected by electroporation with 20 μg of supercoiled CRE expression plasmid pBS185 (Life Technologies). Immediately after transfection, ES cells were plated at various dilutions. From 2 to 12 d after transfection, cells were subjected to gancyclovir selection (2 μM; Syntex, Palo Alto, CA) to enrich for cells that had deleted the marker gene. Surviving clones were picked and analyzed for CRE-mediated recombination by Southern blot analysis of *Bam*HI-digested DNA. Blots were hybridized with probe A (see Fig. 1*A*, *A*).

Four ES cell clones that harbored the targeted locus but lacked the marker gene (F) (see Fig. 1*A*) were injected into C57BL/6J blastocysts to produce chimeric mice. Highly chimeric animals were mated to C57BL/6J females to establish germ line transmission. Heterozygous (F/+) mice of the F1 generation were interbred. Homozygous (F/F) mice were subsequently mated to an actin-CRE general deleter transgenic mouse line on an FVB/N genetic background (Lewandoski et al., 1997) to create the $GABA_A$ receptor α1 null allele (−). Mice that were heterozygous for the α1 null allele (+/−) and positive for the *cre* transgene were mated to mice that were heterozygous for the targeted α1 locus without the marker gene (F/+) and lacked the *cre* transgene. Selected offspring from these matings were used for the experiments reported here. Control animals were α1 homozygous wild type (+/+) with or without the *cre* transgene; knock-out animals were homozygous for the α1 null allele (−/−) and harbored the *cre* transgene. Thus, the mice used for the present studies were of the F4 generation and were composed of a mixed genetic background consisting of C57BL/6J, strain 129/Sv/SvJ, and FVB/N.

Western blot analysis. Western blot analysis of the $GABA_A$ receptor α1 subunit was conducted as described previously (Devaud et al., 1997). In brief, P2 membrane fractions from whole mouse brain were prepared by homogenization in PBS buffer (150 mM NaCl and 10 mM Na_2HPO_4–NaH_2PO_4, pH 7.4). Aliquots of 15 μg/lane protein were separated by SDS-PAGE under reducing conditions using a Novex (San Diego, CA) Xcell II minicell apparatus. Proteins were transferred to polyvinylidine fluoride membranes (Immobilon-P; Millipore, Bedford, MA). Blots were probed with $GABA_A$ receptor anti-peptide α1, amino acid 1–16 (Gao et al., 1993), or actin (Chemicon, Temecula, CA) antibodies. Blots were then probed with horseradish peroxidase-conjugated anti-guinea pig (α1) or anti-mouse (actin) antibodies. Specific peptide labeling was detected by enhanced chemiluminescence (Pierce, Rockford, IL). Blots were apposed to x-ray film under nonsaturating conditions.

Electrophysiology. Sagittal slices of cerebellum (150–200 μm) were prepared from postnatal day 11 (P11) and P35 mice. Cerebellar neurons were viewed with an upright microscope (Axioscope, Zeiss, Germany) equipped with Nomarski optics and an electrically insulated water immersion 60× objective with a long working distance (2 mm). Experiments were performed at room temperature (22–24°C) using an extracellular medium composed of (in mM): 120 NaCl, 3.1 KCl, 1.25 K_2HPO_4, 26 $NaHCO_3$, 5.0 dextrose, 1.0 $MgCl_2$, and 2.0 $CaCl_2$ containing 2 mM kynurenic acid (Aldrich, Milwaukee, WI) to block excitatory amino acid-mediated synaptic transmission. The solution was maintained at pH 7.4 by bubbling with 5% CO_2 plus 95% O_2. The slice was continuously perfused at a rate of 5 ml/min and completely submerged in a total volume of 500 μl. Zolpidem and flurazepam (Sigma, St Louis, MO) were dissolved in dimethylsulfoxide (<0.001% final concentration) and water, respectively, diluted in the extracellular medium, and superfused through a parallel input to the perfusion chamber until effective replacement of the solution was obtained. mIPSCs, a subset of sIPSCs, were recorded in the presence of TTX (1 μM; Sigma).

Cells were accepted as stellate cells only if spontaneous firing of action potentials was observed during seal formation (Llano and Gerschenfeld, 1993; Nusser et al., 1997; Kondo and Marty, 1998). Whole-cell voltage-clamp recordings of sIPSCs and mIPSCs were made with an Axopatch-1D amplifier (Axon Instruments, Foster City, CA), after capacitance and series resistance compensation. Series resistance was typically <15 MΩ and was checked for constancy throughout the experiments. Electrodes were pulled from borosilicate glass capillaries (Wiretrol II; Drummond, Broomall, PA) and were filled with a solution containing (in mM): 145 CsCl, 5.0 EGTA, 5.0 MgATP, and 10 HEPES to pH 7.2 with CsOH. Currents were filtered at 2 kHz with an eight-pole low-pass Bessel filter (Frequency Devices, Haverhill, MA), digitized using a personal computer-compatible microcomputer equipped with a Digidata 1200 data acquisition board (Axon Instruments) and pClamp8 (Axon Instruments) software. Off-line data analysis, curve fitting, and figure preparation were performed with Origin (MicroCal Software, Northampton, MA), pClamp 8.0 (Axon Instruments), and Mini Analysis (Synaptosoft, Leonia, NJ) software. For each cell, mIPSC were averaged from 50 events aligned on the point of steepest rise. Peak amplitudes were measured at the absolute maximum of the currents, taking into account the noise of the baseline and noise around the peak. Rise times were measured as the time elapsed from 10 to 90% of the peak amplitude of the response. Curve fitting was performed using simplex algorithm least squares exponential fitting routines with double exponential equations of the form $I(t) = I_f \exp(-t/\tau_f) + I_s \exp(-t/\tau_s)$, where I_f and I_s are the amplitudes of the fast and slow decay components, and τ_f and τ_s are their respective decay time constants. To compare decay times between different experimental conditions, we used a weighted mean decay time constant $\tau_w = [I_f/(I_f + I_s)] * \tau_f + [I_s/(I_f + I_s)] * \tau_s$. Zolpidem effects were assessed based on averages of 100 sIPSCs in each neuron by statistical comparisons. Unless otherwise indicated, data are expressed as mean ± SEM; *p* values represent the results of independent *t* tests with Bonferroni corrections, or Dunnett's test with prior ANOVA for repeated measures, as appropriate.

RESULTS

Production and characterization of mutant mouse line

A gene targeting construct was used to modify the $GABA_A$ receptor α1 subunit in mouse ES cells, as illustrated in Figure 1*A*. A total of 292 clones were analyzed for gene targeting by Southern blot analysis. After digestion of wild-type ES cell DNA with *Eco*RI, a ~3.2 kb fragment was hybridized with probe C (Fig. 1*A*). Targeting at the α1 locus with the vector resulted in two different targeted alleles depending on where the 3′ crossover occurred. If the crossover event occurred downstream of the 3′-most *lox*P site, that *lox*P site (and accompanying *Eco*RI site) was present at the targeted locus. This allele was detected on Southern blot analysis of *Eco*RI-digested DNA as a ~2.2 kb fragment that hybridized to probe C (Fig. 1*A*, *C*). In contrast, if the 3′ crossover event occurred between the marker gene (i.e., Neo/TK) and the 3′-most *lox*P site, then that *lox*P site was absent from the targeted locus. This allele was detected as a ~8.2 kb *Eco*RI fragment with probe C (data not shown). A total of 19 clones were identified that were correctly targeted that retained the 3′-most *lox*P site, and 16 clones were identified that had lost the 3′-most *lox*P site. The fidelity of targeting was also verified with several additional enzymes and probes (data not shown).

Before using correctly targeted ES cells to create mice, the selectable marker cassette was removed *in vitro* by transient expression of CRE recombinase. ES cell clones that survived gancyclovir selection after transient CRE expression were screened for the desired recombination event by Southern blot analysis. As illustrated in Figure 1*A*, Southern analysis of ES cell DNA digested with *Bam*HI and hybridized with probe A revealed a fragment ~13.0 kb for the wild-type allele (+), ~15.0 kb from the

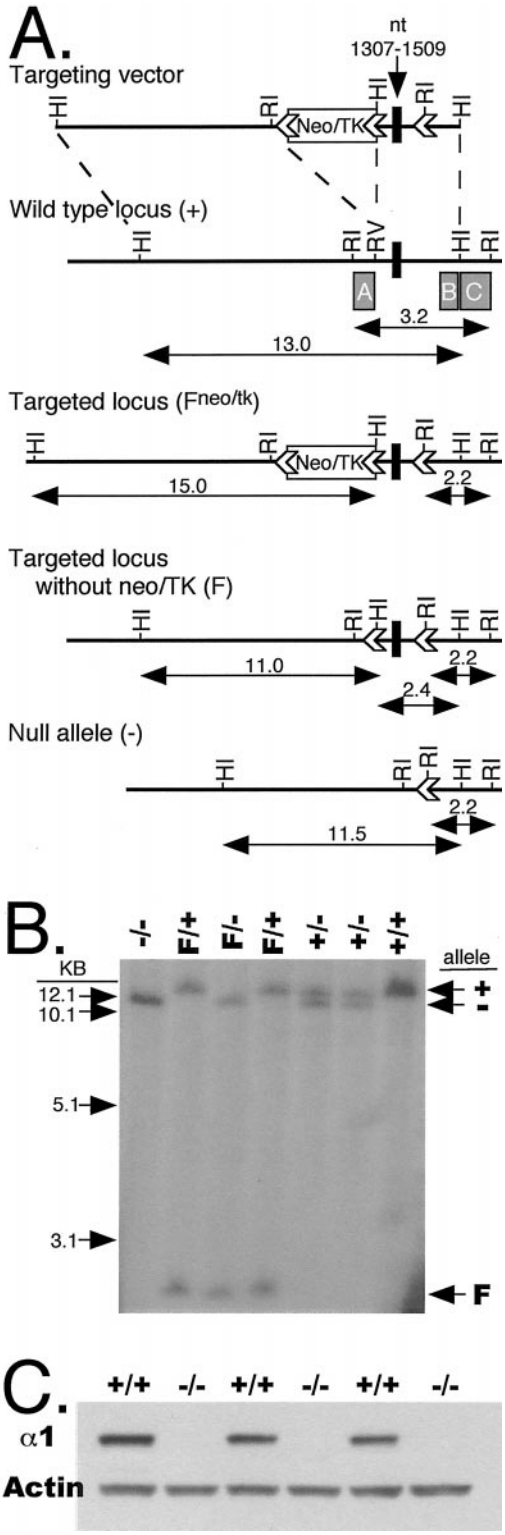

Figure 1. Genetic modification of the α1 subunit of the $GABA_A$-R. *A*, The gene targeting vector was composed of ~13 kb of homologous genomic DNA, the selectable marker gene PGKneoNTRtkpA (*Neo*/*TK*), three *lox*P sites (*arrowheads*), and exonic DNA (*black box*) corresponding to nucleotides 1307–1509 of the $GABA_A$-R α1 subunit cDNA (Keir et al., 1991). *Boxes* labeled *A*, *B*, and *C* under the wild-type locus represent probes used for Southern blot analyses. The wild-type locus (+) was replaced with the targeting construct by gene targeting in mouse ES cells to yield the targeted locus ($F^{neo/tk}$), which contains the marker gene and three *lox*P sites. CRE recombinase was transiently expressed in heterozygous $F^{neo/tk}$ cell lines, and clones in which the marker gene had been successfully removed (F) were identified and injected into blastocysts to make chimeric mice. After germ line transmission of the F allele, mice were mated to a CRE deleter strain (Meyers et al., 1998) to create the recombined, null allele (−). *HI*, *Bam*HI; *RI*, *Eco*RI; *RV*, *Eco*RV. *Arrows* indicate size (in approximate kilobases) of relevant restriction fragments. *B*, Southern blot analysis of mouse tail genomic DNA after digestion with *Bam*HI and hybridization to probe B. *C*, Western blot analysis of mouse brain homogenates using either α1 $GABA_A$-R or β-actin-specific antibodies. Note the complete absence of α1 immunoreactive protein in samples from homozygous null allele (−/−) mice.

targeted locus with the marker ($F^{neo/tk}$), and ~11.0 kb from the targeted allele after CRE-mediated deletion of the marker. Other CRE-mediated recombination events were also distinguished with this same analysis (data not shown). A total of 75 ES cell clones were analyzed, 48 of which harbored the desired recombined locus. We refer to this locus as a floxed locus (F).

Four ES cell clones of the +/F genotype were injected into C57BL/6J blastocysts to make chimeric mice. Two of the four clones yielded highly chimeric mice that transmitted the targeted locus to the next generation. The results presented here were derived from one of the clones (47D12). To convert the F allele to a null allele (−) by recombination of the two remaining *lox*P sites *in vivo*, mice harboring the F allele were mated to a general deleter *cre* transgenic mouse line (Meyers et al., 1998).

All mice were genotyped by Southern blot analysis as illustrated in Figure 1, *A* and *B*. In this analysis, after digestion of genomic DNA with *Bam*HI and hybridization of blots with probe B, the wild-type allele (+) is detected as an ~13.0 kb hybridizing fragment, the null allele (−) as an ~11.5 kb fragment, and the targeted allele without the marker gene (F) as an ~2.4 kb fragment.

The exon deleted by CRE-mediated recombination harbors that part of the gene corresponding to nucleotides 1307–1509 of the α1 cDNA (Keir et al., 1991). These nucleotides are predicted to encode amino acids starting in the putative second transmembrane domain and ending in the intercellular loop between transmembranes 3 and 4. This deletion is also expected to create a frame-shift mutation and prevent the in-frame translation of downstream exons.

To verify that the recombined, null allele was indeed incapable of producing functional α1 protein, Western blot analysis of whole-brain membrane proteins was conducted. As shown in Figure 1*C*, the α1-specific antibody robustly recognized the 51 kDa α1 subunit of the $GABA_A$ receptor in extracts from +/+ mice but failed to recognize any immunoreactive protein in extracts from −/− mice. Thus, the gene targeting event followed by CRE-mediated recombination effectively created a $GABA_A$-R α1 subunit null allele.

Mice that lack the α1 subunit of the $GABA_A$ receptor are viable, healthy, and overtly indistinguishable from their +/+ and +/− littermates. Detailed phenotypic characterization, including whole animal behavioral responses, drug-induced responses, and pharmacology is ongoing and will be reported in a subsequent communication.

Miniature IPSCs in stellate neurons in mice at P11 and P35

sIPSCs were studied in mouse cerebellar slices by means of whole-cell voltage-clamp recordings from granule and stellate neurons, visually identified by their location and morphological characteristics. The average resting potential and input resistance

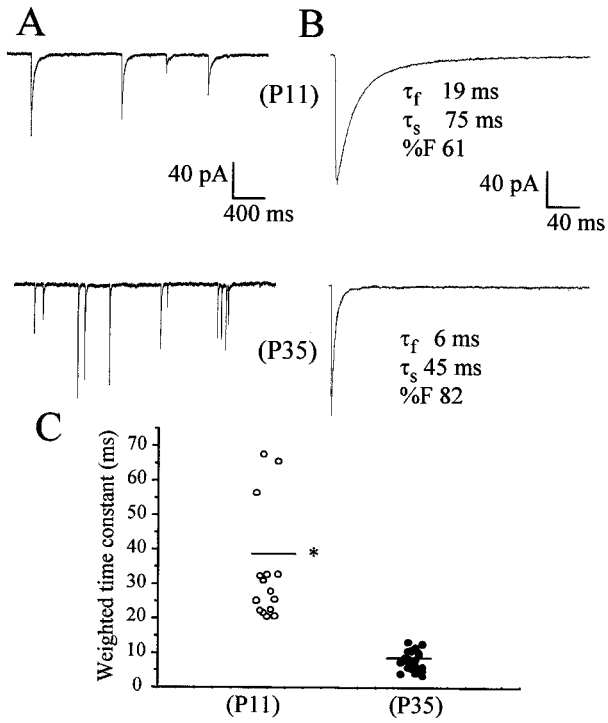

Figure 2. Whole-cell patch-clamp recordings of mIPSCs in stellate cells from mice at P11 and P35. In *A*, the occurrence of mIPSCs, illustrated on a slow time scale in a neuron from a P11 wild-type mouse, is compared with a neuron from a P35 wild-type mouse. In *B*, the average of 50 currents recorded from a single stellate neuron is illustrated with a superimposed double exponential curve with the fast (τ_f) and slow (τ_s) decay time constants indicated and the relative contribution of the fast component to peak amplitude (*%F*). In *C*, the weighted time constant from the exponential fitting of these currents from individual cells is compared between mice at different developmental ages. *Bars* indicate the average values. Data were derived from at least 18 cells from at least five mice in each group. $^*p < 0.01$, statistical significance with respect to P11 mice.

of cerebellar cells were similar (data not shown) to those described previously in rats (Llano and Gerschenfeld, 1993; Brickley et al., 1996; Nusser et al., 1997). Whole-cell recordings of sIPSCs from granule and stellate neurons voltage clamped at −60 mV were performed using an intracellular pipette solution containing 145 mM CsCl and were observed as inward currents. As reported previously (Llano and Gerschenfeld, 1993; Brickley et al., 1996; Nusser et al., 1997), sIPSCs in stellate neurons were larger and more frequent than in granule neurons (data not shown).

We first investigated 18 stellate neurons at P11 from five different +/+ mice and in 25 neurons from six +/+ mice at P35. Spontaneous IPSCs were observed in all stellate neurons, but their frequency of occurrence was highly variable among different cells. mIPSCs were recorded in the presence of tetrodotoxin (1 μM), which depressed the frequency of occurrence of spontaneous IPSCs. mIPSC frequency was 0.47 ± 0.13 Hz at P11 (mean ± SD) and 0.59 ± 0.11 Hz at P35. mIPSCs had a fast rising time (10–90%; 0.7 ± 0.05 msec at P11 and 0.45 ± 0.08 msec at P35), followed by a double exponential decay, as illustrated in Figure 2*B*. The mean amplitude of these events in all cells studied in wild-type mice at P11 and P35 are compared in Table 1. The decay time course of the averaged currents was best fitted by two exponential components (Table 1).

As reported previously, the exponential decay time constants and the fractional contribution to mIPSC peak amplitude of the fast decay component was variable among cells (Nusser et al., 1997). Figure 2*C* is a scatter plot of the weighted time constant of decay of the average mIPSC in each cell studied at the two postnatal ages selected. A statistically significant developmental decrease of the duration of mIPSCs can be observed.

Zolpidem differentially affects mIPSCs in developing stellate neurons

To characterize the relative contribution of α1 subunits of $GABA_A$ receptors in inhibitory synapses of rat cerebellar granule cells during development, we used the imidazopyridine Zolpidem. This compound has been shown to selectively potentiate α1 subunit-containing $GABA_A$ receptor subtypes (Pritchett et al., 1989). As reported previously (Perrais and Ropert, 1999), the effect of Zolpidem on mIPSC peak amplitude relates to the degree of occupancy of postsynaptic GABA receptors. We therefore limited our analysis of the action of the imidazopyridine on the duration of the mISPCs. As illustrated in Figure 3, mIPSCs were recorded in the presence and the absence of Zolpidem. In 12 cells from three +/+ mice at P11, we failed to observe a significant prolongation of mIPSC weighted time constant by two test concentrations of Zolpidem (100 nM and 1 μM) (Fig. 3). In contrast, in 15 cells from six +/+ mice at P35, we observed a statistically significant prolongation of the weighted decay time constant with both concentrations tested (Fig. 3).

mIPSCs in stellate neurons from α1 knock-out mice

We recorded from 18 stellate neurons in four mice at P35 that did not express the α1 subunit of the $GABA_A$ receptor. In two stellate neurons, mIPSCs were not observed. As seen in Figure 4, mIPSCs amplitude was significantly smaller and the decay was significantly longer in neurons from −/− mice. The results obtained are summarized in Table 1. mIPSCs were no different between 25 neurons from six +/+ mice and 14 neurons from five +/− mice at the same age (Table 1). mIPSCs rising time was 0.45 ± 0.08 msec in +/+ mice and 0.59 ± 0.07 msec in −/− mice. Input resistance and cell capacitance were not different in cells from wild-type and knock-out mice, being 0.93 ± 0.22 GΩ and 6.3 ± 1.4 pF for the +/+ mice and 0.98 ± 0.22 GΩ and 6.7 ± 1.2 pF for the −/− mice. We also recorded mIPSCs from six stellate neurons in two −/− mice and from nine stellate neurons in three +/− mice at P11. As seen in Table 1, mIPSCs amplitude was significantly smaller in neurons from −/− mice than in +/− and +/+ mice. In contrast, the decay was not significantly longer in −/− mice (τ_w of 44 ± 6 msec) than in +/+ mice (τ_w of 38 ± 8 msec).

We also investigated the effects of two concentrations of Zolpidem on the duration of mIPSCs recorded in 15 neurons from four −/− P35 mice, 10 neurons from five +/− P35 mice, and 15 neurons from six +/+ P35 mice. As shown in Figure 5, Zolpidem was significantly less efficacious in prolonging the duration of the mIPSCs in stellate neurons from −/− mice. In Figure 5*C*, the summary of the results is reported; the effects of Zolpidem are significant at both concentrations tested for stellate neurons from both +/+ and +/− mice but not in −/− mice. For comparison, we investigated the effect of a nonselective benzodiazepine, flurazepam, on mIPSC recorded in stellate cells from +/+ and −/− mice. In three stellate neurons from two +/+ mice at P35, flurazepam (30 μM) prolonged the weighted time constant of decay by 220 ± 5%, whereas in three stellate neurons from two −/− mice, the prolongation was 240 ± 20%.

Table 1. Characteristics of mIPSCs recorded from developing stellate neuron cerebellar slices

	n cells	Amplitude (pA)	T_{fast} (msec)	T_{slow} (msec)	%Fast
P11					
(+/+)	18	92 ± 18	13.8 ± 1.3*	86 ± 27*	63 ± 8
(+/−)	9	84 ± 14	15.3 ± 2.8*	89 ± 25*	60 ± 5
(−/−)	6	50 ± 15*	15 ± 4.6*	84 ± 19*	56 ± 5
P35					
(+/+)	25	91 ± 15	4.0 ± 0.4	13.2 ± 1.6	62 ± 6
(+/−)	14	106 ± 22	4.1 ± 0.6	14 ± 3	64 ± 5
(−/−)	16	35 ± 6*	16.5 ± 3.1*	75 ± 11*	46 ± 6*

The fractional contribution to peak amplitude and the time constants of the exponential decay component of mIPSCs are compared between cerebellar stellate neurons in different mice. T_{fast} and T_{slow} are the two time constants of the exponential fitting, and %Fast is the relative fractional contribution to the total peak amplitude of the fast decay component. Data are from five (+/+), three (+/−), and two (−/−) mice at P11 and from six (+/+), five (+/−), and four (−/−) mice at P35 from five distinct litters. *$p < 0.05$, statistical significance from the respective value at P35 in +/+ mice (ANOVA followed by Dunnet's test).

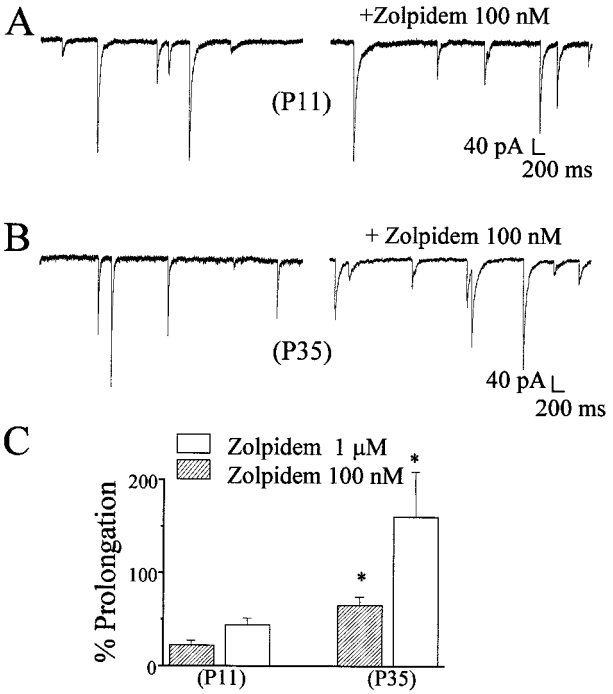

Figure 3. Effects of the imidazopyridine Zolpidem (100 nM) on mIPSCs in cerebellar cells from wild-type mice at P11 and P35. mIPSCs in stellate neurons are illustrated before and after Zolpidem perfusion in a stellate neuron from a P11 mouse (*A*) and a stellate neuron from a P35 mouse (*B*). In *C*, the percentage prolongation of the weighted decay time constants of mIPSCs by two concentrations of Zolpidem is reported for mice at different postnatal ages. Data were derived from at least 12 cells from at least three mice in each group. *$p < 0.05$, significance with respect to P11 mice.

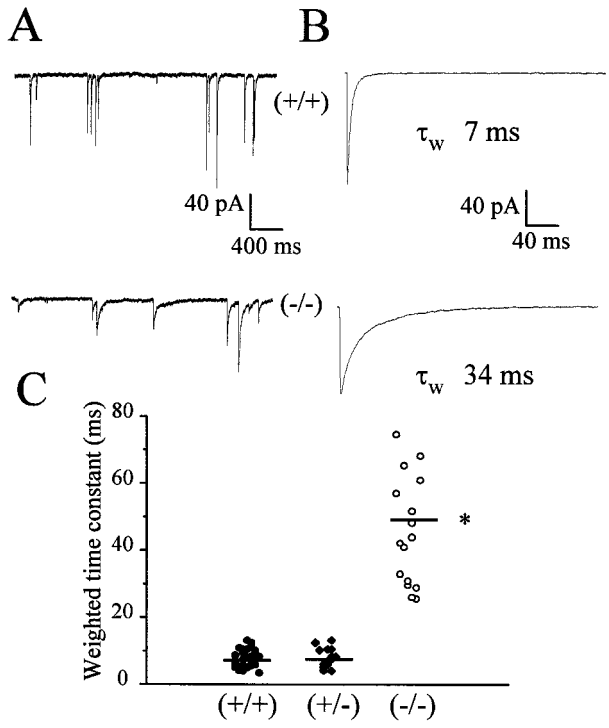

Figure 4. Whole-cell patch-clamp recordings of mIPSCs in stellate cells from genetically altered mice at P35. In *A*, slow sweeps illustrate the occurrence of mIPSCs in a wild-type mouse and in the homozygote α1 −/−. In *B*, the average of 50 currents is illustrated with the weighted decay time constant τ_w from a double exponential curve fit indicated. In *C*, the weighted time constant from the exponential fitting of the currents is compared between different genotypes. *Bars* indicate average values. Data were derived from at least 14 cells from at least four mice in each group. *$p < 0.001$, statistical significance compared with +/+ mice.

sIPSC from granule neurons in α1 deletion mice

As reported previously, TTX (1 μM) strongly depresses the frequency of occurrence of sIPSCs in granule neurons (Brickley et al., 1996; Tia et al., 1996). We therefore studied sIPSCs rather than mIPSCs in granule neurons in cerebellar slices from −/− and +/+ mice at P35. In most neurons from +/+ mice, low-frequency sIPSCs were recorded (10 of 11 cells from four mice). In contrast, in −/− mice, the majority of neurons did not present sIPSCs (four of 16 cells tested from four mice). In those neurons in which sIPSCs were recorded, as can be seen in Figure 6, currents were considerably longer in −/− than in +/+ mice. The summaries of the values of peak amplitude (Fig. 6*D*) and weighted time constants (Fig. 6*E*) characterizing sIPSCs are illustrated. As reported for rats (Brickley et al., 1996; Tia et al., 1996; Wall and Usowicz, 1997), a tonic activation of $GABA_A$ receptors was observed in granule neurons of mice at P35. This was reflected in a considerable baseline noise in whole-cell recordings, which was sensitive to antagonism by bicuculline (Fig. 6*C*), indicating the presence of a considerable amount of ambient neurotransmitter in slices from older animals. However, the extent of the outward current produced in granule cells voltage

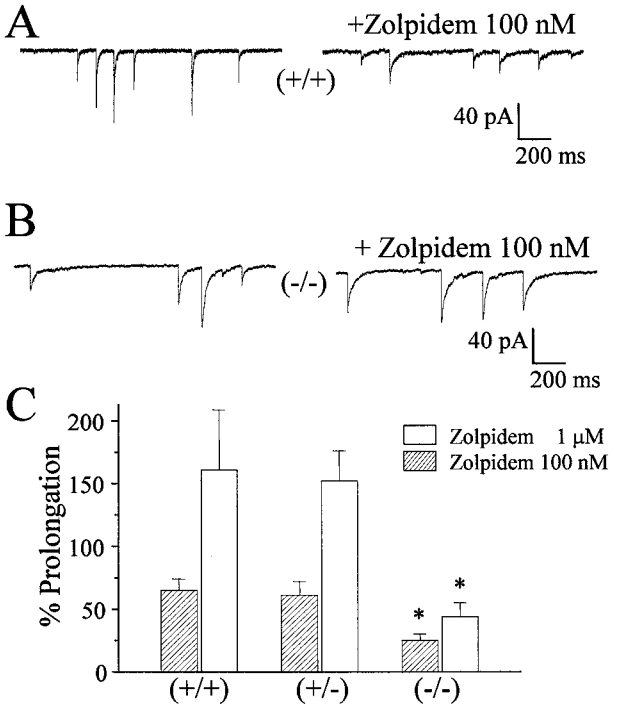

Figure 5. Effects of the imidazopyridine Zolpidem (100 nM) on mIPSCs in cerebellar stellate cells from genetically altered mice. mIPSCs recorded in stellate neurons are illustrated before and after Zolpidem perfusion in a wild-type mouse (*A*) and in a homozygote α1 knock-out mouse (*B*). In *C*, the percentage prolongation of the decay time constants of mIPSCs by two concentrations of Zolpidem is reported for different mice. Data were derived from at least 10 cells from at least four mice in each group. $^*p < 0.05$, significant with respect to +/+ mice.

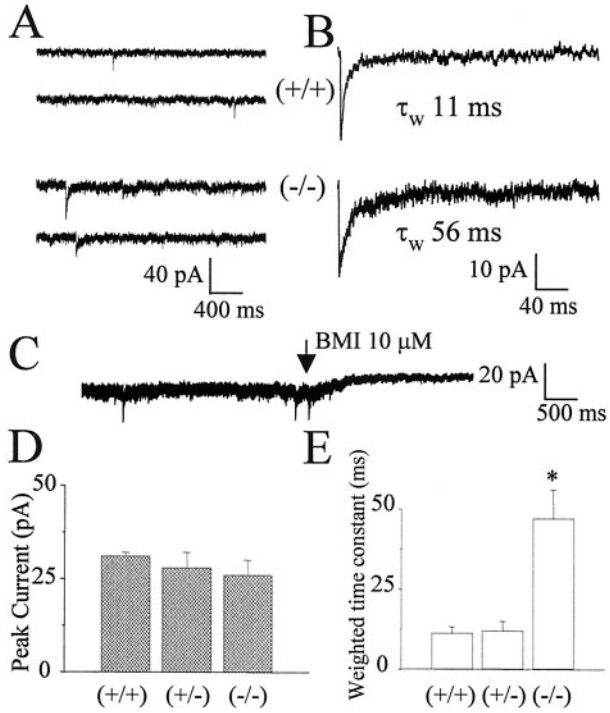

Figure 6. Whole-cell patch-clamp recordings of sIPSCs in cerebellar granule cells from genetically altered mice. In *A*, slow sweeps illustrate the occurrence of sIPSCs in a wild-type mouse (+/+) and in the homozygous α1 knock-out (−/−). In *B*, the average of 50 currents is illustrated. The blockade by bicuculline methiodide (*BMI*) of a background current in a granule neuron from α1 −/− mice at P35 is illustrated in *C*. In *D* and *E*, the peak amplitude and weighted time constant from the exponential fitting of the currents are compared between different genotypes. Data were derived from at least four cells from at least four mice in each group. $^*p < 0.001$, statistical significance compared with +/+ mice.

clamped at −60 mV by the application of bicuculline (5 μM) in +/+ mice did not differ significantly from that measured in −/− mice, respectively, 11 ± 1.2 ($n = 9$) and 12 ± 2.4 ($n = 9$) pA.

DISCUSSION

Several studies have reported developmental shortening of sIPSCs in cerebellar granule cells (Brickley et al., 1996; Tia et al., 1997). In this study, we extend these findings to cerebellar stellate cells and report that these changes are absent in mice with a deletion of the α1 subunit of $GABA_A$ receptors.

The decay of inhibitory currents is regulated in many different ways. Clearance of transmitter from the synaptic cleft (Thompson and Gahwiler, 1992; Draguhn and Heinemann, 1996), multiple vesicle release (Auger and Marty, 1998), and posttranslational mechanisms are all possible determinants of changes in mIPSC decay during development. Our results, however, suggest that the regulation of expression of specific $GABA_A$ receptor subunits with development is conceivably the most important event underlying changes in mIPSC decay. Indeed, in mice at P11 when a low-level expression of the α1 subunit was reported (Laurie et al., 1992b), the difference between mIPSCs decay of wild-type and knock-out mice was not significant.

The hypothesis outlined above requires that various $GABA_A$ receptor subtypes with distinct subunit isoforms have distinct kinetics. Indeed, this has been demonstrated with recombinant $GABA_A$ receptors, in which deactivation of GABA current produced by brief agonist application response is faster when the receptors contain the α1 subunit as opposed to the α2 or α3 subunits (Verdoorn, 1994; Gingrich et al., 1995; Lavoie et al., 1997; McClellan and Twyman, 1999). Shorter GABAergic IPSCs in cerebellar granule cells were proposed to be related to the increased expression of the α6 subunit (Tia et al., 1996). However, the developmental changes also occurred in stellate cells, as reported here, that do not express α6 and in granule cells in mutant mice lacking α6 (Brickley et al., 1999).

These results taken together support our findings and suggest that the developmental increase in α1 subunit expression is responsible for the acceleration of mIPSCs. Previous work related the developmental increase in sensitivity to furosemide to the decrease of mIPSCs duration (Tia et al., 1996). Our results on mIPSCs recorded from granule neurons from α1 knock-out mice suggest that the expression of the α1 subunit is primarily responsible for the developmental decrease of mIPSCs duration. This result together with the developmental increase in sensitivity to furosemide suggest that both α1 and α6 subunits contribute to determine the function and pharmacology of synaptic receptors at inhibitory synapses to cerebellar granule neurons. Indeed, anatomical findings revealed that the α6 and α1 subunits are colocalized in many GABAergic Golgi synapses in granule neurons (Nusser et al., 1998).

Deletion of the α1 subunit causes a significant reduction of mIPSCs amplitude in stellate neurons. This event possibly relates to a decrease in the number of postsynaptic receptors at inhibitory synapses. Surprisingly, this reduction was observed even in −/− mice at P11 when no significant differences in decay kinetics of mIPSCs were seen. The possibility exists that, in wild-type

stellate cells at P11, α1 is normally expressed at a very low level. Lack of even a small amount of α1 could either directly, or indirectly through compensatory changes in levels of other subunits, lead to the observed reduction in mIPSC amplitude. The fact that decay kinetics do not change at P11 in the knock-out may suggest that other subunits are present that have a dominant effect on kinetics and mask the absence of α1 on this parameter at this early age. However, by P35, α1 is normally such an abundant subunit in these cells that its absence is no longer masked.

We did not observe changes in the background current prominent in adult rodent cerebellar granule neurons (Brickley et al., 1996; Tia et al., 1996; Wall and Usowicz, 1997). This indicates that the deletion of the α1 subunit does not affect the expression of $GABA_A$ receptors containing the α6 subunit, which have been reported to be responsible for this background current (Brickley et al., 1999) and to be also located extrasynaptically in these neurons (Nusser et al., 1998).

To support our proposal that the contribution of α1 subunit-containing $GABA_A$ receptors in inhibitory synapses of stellate neurons increases with development, we also studied potentiation of mIPSCs by Zolpidem, an imidazopyridine that has greater potency with $GABA_A$ receptors containing α1 subunits (Pritchett et al., 1989; MacDonald and Olsen, 1994). We showed that Zolpidem did not affect mIPSC decay at P11, although it prolongs the decay rate significantly at P35 in wild-type mice. This implies that $GABA_A$ receptors containing α1 subunits may not contribute to inhibitory synapses before P11. This result matches the developmental expression pattern of the α1 subunit mRNA in the cerebellum (Bovolin et al., 1992; Laurie et al., 1992b) and supports the hypothesis of an increased contribution of the α1 subunit to inhibitory synapses after P11.

What is the subunit composition of GABA receptors in mice that lack the α1 subunit? At the present time, we can only speculate that the expression of other α subunits, such as α5 (Dunning et al., 2000), α2, or α3, may be responsible for slower mIPSCs similar to those found early in development. Indeed, low levels of mRNA for α2 and α3 subunits were seen early in development (Laurie et al., 1992b), and deactivation of GABA responses in cells transfected with these subunits combination is significantly slower (Verdoorn, 1994; Gingrich et al., 1995; Lavoie et al., 1997; McClellan and Twyman, 1999). The prolongation of decay of mIPSCs seen with flurazepam in −/− mice suggests that GABA receptors in these mice are comprised of βγ2 subunits and possibly an α subunit, although potentiation of currents recorded in heterologous cells expressing only βγ subunits has been reported (Sigel et al., 1990; Im et al., 1993). However, the possibility that receptors exclusively assembled with βγ subunits are present in the cerebellum of −/− mice seems unlikely given the low level of expression of receptors with this subunit combination in heterologous systems (Sigel et al., 1990; Verdoorn et al., 1990).

It has been demonstrated that thalamic afferents regulate the area-specific expression of the α1 subunit of $GABA_A$ receptors in developing rat neocortex (Paysan et al., 1997). This raises the intriguing possibility that expression of the α1 subunit is regulated in an activity-dependent manner. Our results would indicate that a reason for the increased contribution of the α1 subunit at inhibitory synapses is to regulate the strength of inhibitory synapses by controlling the duration of IPSCs via the expression levels of this subunit. The experimental verification of this hypothesis is a challenge for the future.

REFERENCES

Auger C, Kondo S, Marty A (1998) Multivesicular release at single functional synaptic sites in cerebellar stellate and basket cells. J Neurosci 18:4532–4547.

Bovolin P, Santi MR, Memo M, Costa E, Grayson DR (1992) Distinct developmental patterns of expression of rat α1, α5, γ2S, and γ2L γ-aminobutyric $acid_A$ receptor subunit mRNAs *in vivo* and *in vitro*. J Neurochem 59:62–72.

Brickley SG, Cull-Candy SG, Farrant M (1996) Development of a tonic form of synaptic inhibition in rat cerebellar granule cells resulting from persistent activation of GABAA receptors. J Physiol (Lond) 497:753–759.

Brickley SG, Farrant M, Wisden B, Cull-Candy SG (1999) The role of α6- and δ-containing $GABA_A$ receptors in the generation of tonic inhibition in cerebellar granule cells. J Physiol (Lond) 518P:140.

Brussard AB, Kits KS, Baker RE, Willems WPA, Leyting-Vermeulen JW, Voorn P, Smit AB, Bicknell RJ (1997) Plasticity in fast synaptic inhibition of adult oxytocin neurons caused by switch in GABAA receptor subunit expression. Neuron 19:1103–1114.

Devaud LL, Fritschy J-M, Sieghart W, Morrow AL (1997) Bidirectional alterations of $GABA_A$ receptor subunit peptide levels in rat cortex during chronic ethanol consumption and withdrawal. J Neurochem 69:126–130.

Draguhn A, Heinemann U (1996) Different mechanisms regulate IPSC kinetics in early postnatal and juvenile hippocampal granule cells. J Neurophysiol 76:3983–3993.

Dunning DD, Hoover CL, Soltesz I, Smith MA, O'Dowd DK (1999) $GABA_A$ receptor-mediated miniature postsynaptic currents and α subunit expression in developing cortical neurons. J Neurophysiol 82:3286–3297.

Farrant M, Wisden W, Cull-Candy S, Brickley SG (1999) Absence of tonic $GABA_A$ mediated conductance in cerebellar granule cells of α6 −/− mice Soc Neurosci Abstr 25:499.6.

Gao B, Fritschy J-M, Benke D, Mohler H (1993) Neuron-specific expression of $GABA_A$-receptor subtypes: differential association of the α1 and α3 subunits with serotonergic and GABAergic neurons. Neuroscience 54:881–892.

Gingrich KJ, Roberts WA, Kass RS (1995) Dependence of the $GABA_A$ receptor gating kinetics on the a-subunit isoform: implications for structure-function relations and synaptic transmission. J Physiol (Lond) 489:529–543.

Hollrigel GS, Soltesz I (1997) Slow kinetics of miniature IPSCs during early postnatal development in granule cells of the dentate gyrus. J Neurosci 17:5119–5128.

Homanics GE, Ferguson C, Quinlan JJ, Daggett J, Snyder K, Lagenaur C, Mi ZP, Wang XH, Grayson DR, Firestone LL (1997) Gene knockout of the α6 subunit of the γ-aminobutyric acid type A receptor: lack of effect on responses to ethanol, pentobarbital, and general anesthetics. Mol Pharmacol 51:588–596.

Im HK, Im WB, Hamilton BJ, Carter DB, Vonvoigtlander PF (1993) Potentiation of gamma-aminobutyric acid-induced chloride currents by various benzodiazepine site agonists with the α1γ2, β2γ2 and α1β2γ2 subtypes of cloned γ-aminobutyric acid type A receptors. Mol Pharmacol 44:866–870.

Keir WJ, Kozak CA, Chakraborti A, Deitrich RA, Sikela JM (1991) The cDNA sequence and chromosomal location of the murine $GABA_A$ α1 receptor gene. Genomics 9:390–395.

Kondo S, Marty A (1998) Synaptic currents at individual connections among stellate cells in rat cerebellar slices. J Physiol (Lond) 509:221–232.

Laurie DJ, Seeburg PH, Wisden W (1992a) The distribution of thirteen $GABA_A$ receptor subunit mRNAs in the rat brain. II. Olfactory bulb and cerebellum. J Neurosci 12:1063–1076.

Laurie DJ, Wisden W, Seeburg PH (1992b) The distribution of thirteen $GABA_A$ receptor subunit mRNAs in the rat brain. III. Embryonic and postnatal development. J Neurosci 12:4151–4172.

Lavoie AM, Tingey JJ, Harrison NL, Pritchett DB, Twyman RE (1997) Activation and deactivation rates of recombinant $GABA_A$ receptor channels are dependent on α-subunit isoform. Biophys J 73:2518–2526.

Lewandoski M, Meyers EN, Martin GR (1997) Analysis of Fgf8 gene function in vertebrate development. Cold Spring Harb Symp Quant Biol 62:159–168.

Llano I, Gerschenfeld HM (1993) Inhibitory synaptic currents in stellate cells of rat cerebellar slices. J Physiol (Lond) 468:177–200.

MacDonald RL, Olsen RW (1994) $GABA_A$ receptor channels. Annu Rev Neurosci 17:569–602.

McClellan AM, Twyman R (1999) Receptor system response kinetics reveal functional subtypes of native murine and recombinant human $GABA_A$ receptors. J Physiol (Lond) 515:711–722.

Meyers EN, Lewandoski M, Martin GR (1998) An Fgf8 mutant allelic series generated by Cre- and Flp-mediated recombination. Nat Genet 18:136–141.

Nagy A, Cocza E, Merenties Diaz E, Prideaux VR, Ivanyi E, Markkula

M, Rossant J (1990) Embryonic stem cells alone are able to support fetal development in the mouse. Development 110:815–821.
Nusser Z, Cull-Candy S, Farrant M (1997) Differences in synaptic GABAA receptor number underlie variation in GABA mini amplitude. Neuron 19:697–709.
Nusser Z, Sieghart W, Somogyi P (1998) Segregation of different $GABA_A$ receptors to synaptic and extrasynaptic membranes of cerebellar granule cells J Neurosci 18:1693–1703.
Okada M, Onodera K, Van Renterghem C, Sieghart W, Takahashi T (2000) Functional correlation of $GABA_A$ receptor subunits expression with the properties of IPSCs in the developing thalamus. J Neurosci 20:2202–2208.
Paysan J, Kossel A, Bolz J, Fritschy JM (1997) Area-specific regulation of gamma-aminobutyric acid type A receptor subtypes by thalamic afferents in developing rat neocortex. Proc Natl Acad Sci USA 94:6995–7000.
Perrais D, Ropert N (1999) Effect of Zolpidem on miniature IPSCs and occupancy of postsynaptic $GABA_A$ receptors in central synapses. J Neurosci 19:578–588.
Pouzat C, Hestrin S (1997) Developmental regulation of basket/stellate cell → Purkinje cell synapses in the cerebellum. J Neurosci 17:9104–9112.
Pritchett DB, Luddens H, Seeburg PH (1989) Type I and Type II $GABA_A$-benzodiazepine receptors produced in transfected cells. Science 245:1389–1392.
Schofield PR, Darlison MG, Fujita N, Burt DR, Stephenson FA, Rodriguez H, Rhee LM, Ramachandran J, Reale V, Glencorse TA, Seeburgh PH, Barnard EA (1987) Sequence and functional expression of the GABA A receptor shows a ligand-gated receptor super-family. Nature 328:221–227.
Sigel E, Baur R, Trube G, Mohler H, Malherbe P (1990) The effect of subunit composition of rat brain $GABA_A$ receptors on channel function. Neuron 5:703–711.
Sternberg N, Hamilton D (1981) Bacteriophage P1 site-specific recombination. I. Recombination between loxP sites. J Mol Biol 150:467–486.
Thompson SM, Gahwiler BH (1992) Effects of the GABA uptake inhibitor tiagabine on inhibitory synaptic potentials in rat hippocampal slice cultures. J Neurophysiol 67:1698–1701.
Tia S, Wang JF, Kotchabhakdi N, Vicini S (1996) Developmental changes of inhibitory synaptic currents in cerebellar granule neurons: role of $GABA_A$ receptor α6 subunit. J Neurosci 16:3630–3640.
Verdoorn TA (1994) Formation of heteromeric γ-aminobutyric $acid_A$ receptors containing two different α subunits. Mol Pharmacol 45:475–480.
Verdoorn TA, Draguhn A, Ymer S, Seeburg PH, Sakmann B (1990) Functional properties of recombinant rat $GABA_A$ receptors depend upon subunit composition. Neuron 4:919–928.
Wall MJ, Usowicz MM (1997) Development of action potential-dependent and independent spontaneous $GABA_A$ receptor-mediated currents in granule cells of postnatal rat cerebellum. Eur J Neurosci 9:533–548.
Wu H, Lin X, Jaenisch R (1994) Double replacement: strategy for efficient introduction of subtle mutations into the murine Col1a-1 gene by homologous recombination in embryonic stem cells. Proc Natl Acad Sci USA 91:2819–2823.